Recognition of Motion Blurred Iris Images

Jing Liu[1,2], Zhenan Sun[2], Tieniu Tan[2]
1. Department of Automation, University of Science and Technology of China
2. Center for Research on Intelligent Perception and Computing,
National Laboratory of Pattern Recognition, Institute of Automation,
Chinese Academy of Sciences, P.O. Box 2728, Beijing, P.R. China, 100190
liujing0@mail.ustc.edu.cn, {znsun,tnt}@nlpr.ia.ac.cn

Abstract

It is inevitable to capture a portion of iris images with motion blur during iris recognition. The texture details on iris patterns are lost in motion blurred images so it may cause recognition performance degradation. This paper presents a first systematic study on the issue of motion blurred iris image recognition. Firstly, the reason of generating motion blurred iris images is analyzed. Secondly, the influence of the strength and the direction of motion blur on the accuracy of iris recognition is quantitatively investigated. Thirdly, we propose two solutions which can be used separately or jointly to improve recognition accuracy on motion blurred iris images. The first solution is a deblurring method in preprocessing stage and the other is a motion blur weight map with two generation methods in matching stage. Experimental results on both synthetic and real-world motion blurred iris image databases demonstrate the effectiveness and efficiency of our methods.

1. Introduction

Recognition of motion blurred iris images is an inevitable problem in iris biometrics. There are three parts in a systematic study of motion blurred iris image recognition as shown in Figure 1. This issue is not well addressed in the literature. Because the fundamental part, i.e., the influence of motion blur on iris recognition performance has not been quantitatively investigated and analyzed in details. Moreover, the current solutions to motion blurred iris image recognition usually follow an intuitive idea, i.e., restoring images [15] before recognition. In current iris image deblurring methods, blurring kernels are always assumed to follow parametric models, which is too simplified for the real world motion blur. Apart from image deblurring, there is actually another approach to this problem. It is to develop a feature extraction algorithm or a matching strategy which is robust to motion blurred iris images. Therefore, the extracted features or the generated matching scores can be less influenced by motion blur. They can be not only used separately but also incorporated with a restoration method for further performance improvement.

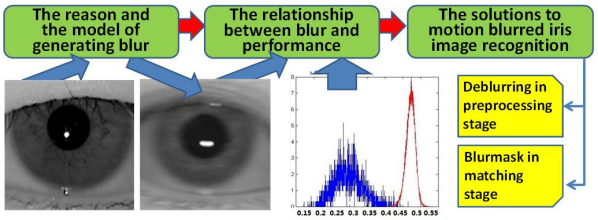

Figure 1. Three parts of the systematic study of motion blurred iris image recognition.

This paper aims to present a systematic study on recognition of motion blurred iris images. Firstly, the reason and model of generating motion blurred iris images are analyzed. Secondly, the relationship between iris image blurring and iris recognition performance is investigated and its primary explanations are also provided. They are treated as the foundation of our proposals for recognizing motion blurred iris images. Thirdly, we propose a novel Matching Scheme incorporating Deblurring and Blurmask (MSDB) as a comprehensive solution for motion blurred iris image recognition. MSDB is conducted in two stages, i.e., image restoration in the preprocessing stage and a blurmask strategy in the matching stage. Our deblurring method takes advantages of both the two-phase structure and the distinctive characteristics of iris images. It is performed in the selected filter domain rather than the pixel domain, which guarantees efficiency and robustness. Meanwhile, the blurmask adaptively weights each bit in iris code based on its blur situation instead of directly discarding the unreliable regions with information loss. From different perspectives, two mask generation methods are proposed according to whether there

are available training samples. Experiments on both synthetic and real-world databases show that these two solutions of MSDB can be used separately or jointly to improve recognition performance on motion blurred iris images.

The remainder of this paper is organized as follows. In Section 2 background is introduced. In Section 3 the influence of motion blur on iris recognition is studied. Section 4 and Section 5 present preprocessing-level and matching-level solutions to recognizing motion blurred iris images respectively. The experimental results are illustrated in Section 6. Section 7 concludes this paper.

2. Background

Given a clear image I, space-invariant blurring can be modeled as a convolution process [9],

$$B = I \otimes f + n, \tag{1}$$

where B and n represent the blurred image and additive noise, respectively. $\otimes$ denotes the convolution operator, and f is the point spread function (PSF), namely blurring kernel. Its inverse procedure is the deblurring problem which can be optimized by alternatively solving the equations as [3]

$$\hat{f} = \arg\min_{f} \Phi(I \otimes f - B) + \alpha\Theta_1(f), \tag{2a}$$

$$\hat{I} = \arg\min_{I} \Phi(I \otimes f - B) + \beta\Theta_2(I), \tag{2b}$$

where $\Phi(I \otimes f - B)$ is the fidelity term, $\Theta_1(f)$ and $\Theta_2(I)$ denote the regularization terms on f and I, respectively. α and β are the regularization parameters.

2.1. Related work

Nature-scene deblurring methods have been extensively investigated in the literature, however directly using them on blurred iris images can not guarantee the performance improvement due to the unique characteristics of iris images. To this end, some restoration algorithms [13, 14, 15, 18] are proposed particularly for iris images. Among them, the parametric model of motion blur is defined as

$$f_{mot}(x, y) = \begin{cases} \frac{1}{d} & \text{if } x^2 + y^2 < d^2 \text{ and} \\ & \quad x\sin(\theta) = y\cos(\theta) \\ 0 & \text{otherwise,} \end{cases} \tag{3}$$

where θ and d represent the direction and the length of motion blur, respectively. This fixed kernel form is always too specific to characterize the actual blurring reasons resulting in degraded outputs. Even worse, the parameters are basically estimated from visual appearances, which not only narrows the range of applications but also brings down the reliability.

The robust feature extraction methods for iris recognition have been widely studied, while not enough attention is paid to the feature matching with weight maps in the literature [7, 12]. These weighting strategies are supposed to mainly focus on the quantization error [7] and personality [12] rather than low-quality iris images.

3. A study of the influence of motion blur on iris recognition performance

In this section, we discuss the relationship between blurring situation and recognition accuracy, which is not only essential but also very helpful in developing a robust matching scheme against motion blur. To fully exploit this potential relationship, experiments on both synthetic and real-world datasets are conducted in the following sections.

3.1. Iris recognition performance as a function of the strength of motion blur

To report real-world performance, genuine iris image databases with motion blur which are detailed in Section 6 are applied for the evaluation, and the results are shown in Figure 3 (a). It is clear that recognition performance with presence of motion blur drops significantly. However, it is challenging to separately investigate the influence of motion blur strength and orientation on recognition performance, because motion blurred iris images with controlled parameters can be hardly captured. Therefore, it is better to synthetically generate blurred iris image datasets to quantitatively investigate the degradation of iris recognition performance with motion blur. We select 1,214 clear iris images $I^i(x, y), i = 1, 2, \ldots, 1214$ from ICE [1] for this assessment. ICE database [1] is applied because it almost only contains one covariate, namely defocus blur which can be easily eliminated via focus value estimation [6]. By the nature of blurring model in Equation (1), I^i is artificially blurred by convolving with the desired PSFs, as $I^i \otimes f_{mot}$. Afterwards, it is localized and normalized ($NOR(\cdot)$) into y_{max} (height) $\times$ x_{max} (width). This type of blur generation $I_{NB} = NOR(I^i \otimes f_{mot})$ simulates the distortion in real world, and is denoted as Type 2 blur generation which is red in Figure 2. The examples of unwrapped original image $NOR(I^i)$ and I_{NB} are shown in Figure 2 (a) and (c).

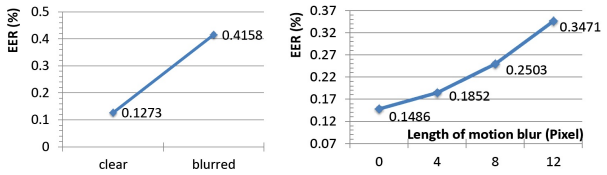

Figure 3. (a) Experimental results without and with motion blur on real-world datasets. (b) Experimental results with increasing degree of motion blur on synthetic datasets.

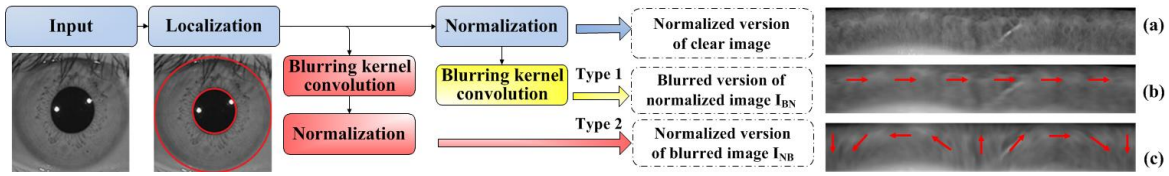

Figure 2. The flowchart of two types of blur generation for iris images. (a) A normalized clear iris image. (b) Type 1. Synthetic blur on normalized image, I_{BN} with $\theta = 0$. (c) Type 2. A normalized version of blurred image, I_{NB} with $\theta = 0$.

The applied iris recognition algorithm is based on ordinal measures (OM) [20] which are state-of-the-art image descriptors for encoding discriminative features of iris images. Equal error rate (EER) refers to the point in receiver operating characteristic (ROC) curve when false accept rate (FAR) is equal to false reject rate (FRR). It is employed as the quantitative measurement of iris recognition performance. Iris recognition performance as a function of the strength of motion blur is shown in Figure 3 (b). The experimental results show that motion blurred iris images degrade recognition performance more significantly with the increasing of d.

3.2. Iris recognition performance as a function of the orientation of motion blur

To directly investigate the performance variation in term of θ in a quantitative way, blur is synthesized after normalization $I^i_{BN} = f^{\theta}_{mot} \otimes NOR(I^i)$, which is the Type 1 of blur generation shown in Figure 2. The applied PSFs f^{θ}_{mot} have a fixed length d and different θ. An example with $\theta = 0$ can be found in Figure 2 (b). The recognition results with different directions of motion blur are illustrated in Figure 4 (a). Here, the blue dotted line indicates the recognition result of selected clear images, meanwhile the red solid line corresponds to the experiments by using the generated datasets with different f^{θ}_{mot}. Some observations and analyses are provided as follows.

Observation 1. It can be seen that recognition accuracy varies according to different motion directions even if d is fixed. The explanations are as follows: The distinguishable information of a normalized iris image is mostly conveyed in horizontal direction rather than vertical direction. Therefore, when the orientation of motion blur is close to $0°/180°$, the preserved information of an iris image will be damaged dramatically resulting in a sharply decreasing recognition accuracy.

Observation 2. Blur makes different influences on genuine and imposter matching. 1) Blur aggravates the variations of different images captured from the same iris. It enlarges the dissimilarities between intra-class samples. A validation can be found from the experimental results shown in Figure 4 (b), where the mean value of genuine matching distances changes with different θ. 2) Although the mean value of imposter matching distances is stable, their distribution is found to be flattened when motion blurred iris images are used, as shown in Figure 4 (c) and (d). The larger deviation indicates a smaller (degrees-of-freedom) DOF [5], which means that the uniqueness of our iris code is undermined causing performance degradation. The nature of blurring model in Equation (1) takes responsibility for this observation, because the convolved pixels are essentially determined by its neighboring regions causing the increased inherent correlations within an iris code.

4. Iris image deblurring

In this section, a deblurring algorithm is developed as the solution in preprocessing stage. It employs a coarse-to-fine framework including coarse kernel estimation and image deblurring, where PSF is modeled on parametric-level and pixel-level respectively. This combination brings in the advantages of both models, i.e., simplicity and accuracy. The coarse estimation provides a reasonable starting point and helps image restoration apart from computationally expensive iterations. Although it can be hardly obtained in nature scene applications due to the limited prior information, the distinct characteristics of iris images facilitate this coarse estimation in our application. In image deblurring, reliable region detection (RRD) makes full use of the particular analysis of iris images. Compared with nature-scene deblurring methods, RRD-based algorithm in filter domain [8] ensures higher levels of efficiency and reliability.

4.1. Framework

Since the initialized PSF will be subsequently refined, the parametric kernel model is first adopted with the emphasis on efficiency. It turns coarse kernel initialization into the determination of θ and d in Equation (3). From Figure 1, it is apparent that the shape of reflection on pupil generally reveals the blurring reason. Therefore, this morphology information is applied to determine the motion blur parameters via directional filters and pre-trained relationships between lengths of reflection and motion blur. Actually, the shape information of corneal reflections is widely adopted in iris recognition applications and also theoretically analyzed in [10]. Even if the reflection-based method fails in some applications, I-IQA [17] can also be applied as substitution.

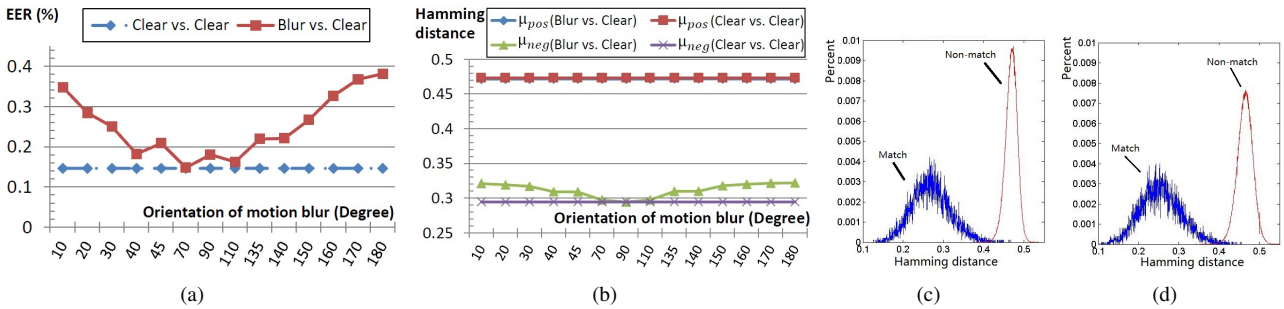

(a) (b) (c) (d)

Figure 4. (a) Recognition results with different directions of motion blur. (b) Varying mean values of genuine and imposter matching distances (where $\mu_{pos}(Blurvs.Clear)$ are occluded by $\mu_{pos}(Clearvs.Clear)$). (c) The distributions of genuine and imposter matching distances on clear iris images. (d) The distributions of genuine and imposter matching distances on blurred iris images.

After initialization, PSF turns to be modeled on pixel-level rather than characterized by θ and d, thus its form is flexible enough to truly express the blurring reason. Traditional deblurring methods always predict the clear image by using complicated prior and exclude the detrimental structures [4] in an iterative way. These two kinds of optimizations are actually guessing procedures which not only are time consuming but also inevitably introduce spurious information. However, reliability and efficiency are significant for iris recognition. We solve this problem by means of detecting the reliable regions in the filter domain to guide the alternative optimization of I and f.

4.2. Deblurring based on reliable region detection

The outliers are pixels which can not be modeled as Equation (1), thus they certainly deteriorate image deblurring based on this model. In iris images, they principally consist of the overflow regions due to the saturated intensities. Although they can be easily excluded in PSF estimation, severe ringing artifacts will be presented in the estimated clear image [4]. Fortunately, overflow regions in iris images can be filled by specular reflection removal method [11]. Afterwards, reliable region detection is applied to find the regions benefitting kernel estimation. The estimation in filter domain is more efficient [8], which encourages the use of gradient images for RRD. Significant edges are helpful to estimate the PSF [16], but two edges within a smaller distance than the scale of PSF will increase the estimation ambiguity. That is to say the elements with large gradient except the regions of dense and multiple edges, i.e., eyelashes regions in iris images, are suggested to be selected into the set S_{fd}^{i+1} in $(i+1)$-th iteration as $RRD_{fd}(I): S_{fd}^{i+1} \leftarrow \{j : k_j^i > t^s \bigcap mask_j = 1\}$, where j indexes the gradients k^i of I. t^s is configured by applying the quartile to form the partial support. $mask$ denotes the segmentation result [11] indicating eyelids.

With the detected regions $RRD_{fd}(I)$, the reliable regions in blurred image B is selected by marking large-value elements in the convolution of I and f, as $RRD_B(B): S_b \leftarrow \{j : (I \otimes f)_j > th\}$. Since iris image segmentation and reflection removal [11] are robust and necessary for recognition, RRD can improve restoration reliability without sacrificing efficiency.

Given the selected regions by RRD, the filter domain estimation is applied to totally capture the spatial randomness of noise [19]. After iterations, the final restored image can be obtained by alternatively optimizing Equation (2). The fidelity term $\Phi(I \otimes f - B)$ in Equation (2) can be rewritten into

$$\Phi = \sum_i \omega_i \| RRD_I(\partial_i I) \otimes f - RRD_B(\partial_i B) \|^2, \quad (4)$$

where $\partial_i \in \{\partial_x, \partial_y, \partial_{xx}, \partial_{yy}, \partial_{xy}\}$ and $\omega_i \in \{\omega_x, \omega_y, \omega_{xx}, \omega_{yy}, \omega_{xy}\}$ denote the partial derivative operator and weight in different directions and orders. The regularization terms of f and I take the forms of $\|\triangle f\|^2 = \|f_i - f_{i-1}\|^2$ and $\|\nabla I\|^2$, respectively.

5. Matching strategy based on blurmask

The increasing tendency of inherent correlations within iris code can be alleviated after restoration, since the blurred iris images are deconvolved. However, some images degraded by large PSF still can not be totally restored. The results to be presented in Section 6 show the performance after restoration still has potential to be further improved. It is undoubtedly a support to the requirement of an advanced matching strategy as a complementary solution to the problem of motion blurred iris image recognition.

Iris feature codes are usually represented using binary strings. As a traditional dissimilarity measurement, Hamming Distance HD between a registered iris code $code_X$ and a query iris code $code_Y$ is written as

$$HD_{AB} = \| \ XOR(Code_X, Code_Y) \ \|, \quad (5)$$

where XOR is the exclusive-OR operator. This matching strategy treats the iris texture patterns with different motion

situations equally, however recognition accuracy varies in term of motion blur direction. Therefore, it is certainly not optimal for matching motion blurred iris images. The improvement of blurmask BM_Y for the query iris code $code_Y$ is to adaptively set each bit a weight according to its blurring situation. Since the registered $code_X$ is usually derived from an image of high quality, only BM_Y is introduced to the matching function as follows:

$$HD_{AB} = \| \ XOR(Code_X, Code_Y) \times BM_Y \ \|, \quad (6)$$

Before the calculation of blurmask, the blurring information θ and d are firstly updated by using the directional filters and measuring the length along main direction on the refined PSF, since the initial PSF characterized by θ and d has been refined on pixel level. Afterwards, the updated θ and d are applied to generate a blurmask dealing with the remained blurred texture patterns. The way to generate blurmasks is the key issue of this section. Depending on whether training samples are used, two different methods are proposed and will be detailed in the following sections.

5.1. Heuristic blurmask generation

Observation 1 in Section 3 reveals that the horizontally blurred region (REG_{hb}) dramatically degrades recognition performance, thus they are expected to be marked before the subsequent processes. With REG_{hb}, a heuristic method is proposed to automatically generate the blurmask without training samples denoted as "blurmask-h".

In Figure 2 (b) and (c), the directions of red arrows generally show the directions of motion blur suffered by the corresponding regions. It is apparent that the direction of PSF in an unwrapped image I_{NB} varies regularly with the horizontal coordinate. Theoretically, this varying pattern is determined by the normalization method adopted in a recognition system. Based on this relationship as well as the motion parameters $\theta \in [0, \pi]$ and d on the original image, the calculation of $REG_{hb}^{\theta,d}$ can be written as

$$\begin{aligned} REG_{hb}^{\theta,d} = &[\frac{\theta_0+\theta}{2\pi}y_{max} - w_d, \frac{\theta_0+\theta}{2\pi}y_{max} + w_d] \\ \cup &[\frac{\theta_0+\theta+\pi}{2\pi}y_{max} - w_d, \frac{\theta_0+\theta+\pi}{2\pi}y_{max} + w_d], \end{aligned} \quad (7)$$

where $w_d = w + d/2$ and the blurmask window $w \in (0, y_{max}/4)$ is half of the blurmask size. θ_0 is the starting angle in iris normalization methods, and it is $\pi/2$ in our implementation. Here, the horizontal coordinate y in normalized image is treated circularly, i.e., $I_n(x, y_{max} + y) = I_n(x, y)$. The heuristic blurmask BM_h is generated from the consideration of adaptively strengthening the penalties of unmatched pixels in REG_{hb}. It is defined as

$$BM_h(x,y) = \begin{cases} \alpha_{\theta,d}(x,y) & (x,y) \in REG_{hb}^{\theta,d} \\ 1 & others, \end{cases} \quad (8)$$

where $\alpha_{\theta,d}(x, y)$ is the penalty coefficient. It can be determined by a variety of considerations resulting in the generalization of MSDB.

5.2. Training-based blurmask generation

Compared with blurmask-h, the generation method presented in this section can get rid of finding REG_{hb} and designing the penalty coefficient of blurmask when there are available training samples. This method is proposed from the perspective of iris code inconsistence [12], the general stability map P is first calculated and then used to automatically generate the training-based "blurmask-t".

Due to the presence of motion blur in iris images, the stability of iris feature codes decreases. Especially, the bits with horizontal blur turn to be fragile, i.e., their codes frequently change in different images of the same iris. Suppose $I^i, i = 1, 2, \ldots, N$ are training iris images belonging to classes $C_1, C_2, \ldots, C_{N_c}$, and their iris codes are denoted by $code_{I^1}, \ldots, code_{I^N}$. Following the second type of blur generation, we artificially blur I^i and obtain I^i_{NB} with $\theta = 0$ and $d = 15$. An example can be found in Figure 2 (c). The samples in the same class with different blurring situations are matched, and their average result is

$$P = \frac{1}{\alpha}\Sigma_{k=1}^{N_c}\Sigma_{i,j\in c_k}\overline{XOR(code_{I^i}, code_{I^j_{NB}})}, \quad (9)$$

where $\alpha = \Sigma_{k=1}^{N_c} Num^2(C_k)$, $Num(C_k)$ is the number of images in class C_k. As illustrated in Figure 5, P is the general stability map with the same size as iris codes. The bright area in P indicates the reliable region while the matching results in the dark area are less stable. The bright and the dark areas are alternatively distributed with a regular pattern. Compared with Figure 2 (c) and Figure 5, the dark areas in P are found to share a similar existing pattern with the heuristically designed REG_{hb}.

Figure 5. The calculated stability map P of iris feature bits.

The stability map P is more precise than REG_{hb} and is always between 0.5 and 1. To set each coding bit a suitable penalty based on its stability, we normalize and rotate the general P to calculate the training-based blurmask BM_t as

$$BM_t(x,y) = \frac{\alpha_{max} - 1}{P(x, y + \frac{\theta}{2\pi}y_{max})} - \alpha_{max} + 2, \quad (10)$$

where α_{max} is the max penalizing value giving the most severe punishment for unreliable iris feature bits, and the horizontal coordinate y is also treated circularly. In this way, $\alpha(x, y)$ is proportional to $1/P(x, y)$ and belongs to

$[1, \alpha_{max}]$. The obtained blurmask is actually $BM_t^{d=15}$, thus a few experiments with motion length $d = 5, 10, 20$ are required for the whole BM_t which can cover a wide range of blur.

6. Experiments

In this section, the parameters in MSDB are firstly discussed and set window size $w = 24$, penalizing coefficients $\alpha = 1.25$ and max penalizing value $\alpha_{max} = 1.4$ respectively. Afterwards, the deblurring method and the blurmask strategy in MSDB are separately compared with the previous iris image deblurring methods to demonstrate the effectiveness of our proposed algorithms. Finally, the deblurring method and blurmask are combined into the unified MSDB to verify the further improvement of recognition accuracy.

6.1. Experimental results

Two solutions in MSDB, i.e., restoration and blurmasks, are firstly compared with the existed deblurring methods respectively, and then they are integrated as the whole MSDB to show the further improved recognition performance. As a common criteria, discriminating index (d') is applied to represent the separability of genuine and impostor distributions. It is defined as

$$d' = |\mu_{pos} - \mu_{neg}| / \sqrt{(\sigma_{pos}^2 + \sigma_{neg}^2)/2}, \qquad (11)$$

where μ_{pos}, σ_{pos}, μ_{neg} and σ_{neg} represent the means and standard deviations of genuine and imposter matching distributions, respectively.

Synthetic dataset. The previously selected clear images $I^i(x, y)$, $i = 1, 2, \ldots, 1214$ in ICE [1] are also applied in this experiment. PSFs with $\theta \in [0, \pi]$ and $d \in [5, 20]$ are randomly generated to artificially synthesize motion blurred databases based on the second type of blur generation approach. The clear database is used for enrollment, while blurred images are used for test, denoted as *Baseline*. As comparisons, the images deblurred by [15] [18] are applied to match the registered iris images. They are denoted as *Deblur-[15]* and *Deblur-[18]*. The results by using our proposed deblurring method and blurmask-h/t are denoted as *Deblur-our* and *Blurmask-h/t*. Specially, the results of integrated MSDB, i.e., the integration strategy of our proposed deblurring method and blurmask-t are also evaluated to verify the further improvement, called *Deblur-our + Blurmask-t*. To estimate the general stability map P, 214 images are randomly selected as training samples from the original clear database. These experimental results are illustrated in Table 1 and Figure 6 (a).

Table 1. Comparison of recognition performance on the synthetic and the real-world datasets.

		Synthetic data		Real-world data	
		EER (%)	d'	EER (%)	d'
Baseline		0.391	5.058	0.113	4.881
Deblurring	Kang [15]	0.306	5.187	0.104	4.899
	Liu [18]	0.246	5.702	0.060	5.291
	Our	**0.230**	**5.723**	**0.051**	**5.311**
Blurmask-h		0.228	5.721	0.095	5.044
Blurmask-t		0.217	5.730	0.091	5.064
Deblur-our+Blurmask-t		**0.163**	**5.831**	**0.045**	**5.324**

Real dataset. Although there are some databases released for the study of iris recognition. To the best of our knowledge, it is difficult to find a public iris image database that contains only motion blur with no other covariates. Therefore, two databases are collected by ourselves to conduct the succeeding experiments. IrisGuard H100 [2] is used for data acquisition in our experiments. The first database contains 266 iris images with different degrees of motion blur, while the second one contains 141 clear iris images captured from the same eyes in the first database. The experiments on real-world databases are conducted with the same consideration as the above experiment on synthetic examples. The randomly selected 41 clear images are served as training samples for BM_t.

From the results shown in Table 1 and Figure 6, several observations can be drawn. 1) Our proposed deblurring method outperforms the previous methods in terms of both EER and d', since pixel-level PSF model is applied after initialization and the distinctive prior information of iris images is exploited. 2) The proposed matching strategy based on blurmasks improves iris recognition performance, which validates the effectiveness of blurmask. The reliability of blurmask is guaranteed by the usage of observed blurring patterns rather than the fragile prior information in restoration methods. Since the stability map P is used, the training-based blurmask-t is more precise than blurmask-h, resulting in a larger performance improvement. 3) The recognition performance can be further enhanced when blurmasks are incorporated with the deblurring methods. It means that the above two solutions not only achieve the ultimately same goal by different routes so as to make the recognition system more tolerant to motion blur, but also are complementary to each other. Additionally, the computational cost of blurmask is not obviously increased compared with the single restoration algorithm since the motion direction and length are already identified for restoration. Therefore, the integrated MSDB is suggested to be incorporated into practical recognition systems in less-intrusive environments.

7. Conclusions

In this paper, a systematic study on recognition of motion blurred iris images has been presented. The influence of motion blur for iris recognition is further exploited. The basic pattern of how and why motion blurred iris images de-

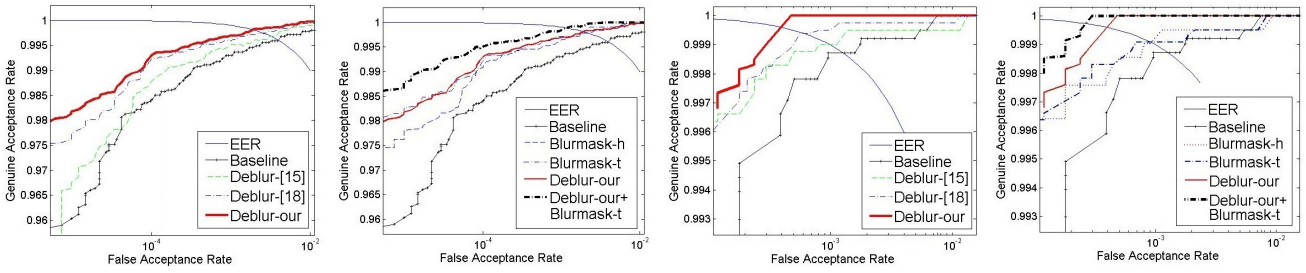

(a) (b) (c) (d)

Figure 6. Comparison of the proposed deblurring algorithm with the existing deblurring methods [15] [18] on (a) the synthetic and (c) the real-world datasets. Comparison of the proposed blurmasks-h/t with the integration strategy of our proposed deblurring algorithm and blurmask-t on (b) the synthetic and (d) the real-world datasets.

grade recognition performance are analyzed by conducting a series of experiments, and their intuitive interpretations are also provided. Based on these observations, a novel Matching Scheme incorporating Deblurring and Blurmask (MSDB) is proposed to improve the recognition accuracy on motion blurred iris images. It is implemented in both preprocessing and matching stages. The motion blurred iris images can be firstly enhanced, and then their unreliable regions are marked and penalized strictly with the proposed matching strategy. To the best of our knowledge, our work is the first comprehensive research of motion blurred iris image matching which contains the three essential parts for systematic studies. In the future, we plan to develop a more efficient form of penalty function, and this procedure may be explicitly modeled as an optimization problem. In addition, it is of interest to develop the matching strategies for other covariates, e.g., out-of-focus and off-angle.

8. Acknowledgement

This work is funded by National Natural Science Foundation of China (Grant No. 61075024, 61273272), International S&T Cooperation Program of China (Grant No.2010DFB14110).

References

[1] ICE. `iris.nist.gov/itl/iad/ig/iris.cmf`.

[2] IrisGuard H-100. `www.irisguard.com`.

[3] S. Cho and S. Lee. Fast motion deblurring. In *ACM Trans. on Graphics*, volume 28, page 145. ACM, 2009.

[4] S. Cho, J. Wang, and S. Lee. Handling outliers in non-blind image deconvolution. In *ICCV*, pages 495–502. IEEE, 2011.

[5] J. Daugman. High confidence visual recognition of persons by a test of statistical independence. *IEEE Trans. on Pattern Anal. Mach. Intell*, 15(11):1148–1161, 1993.

[6] J. Daugman. How iris recognition works. *IEEE Trans. on Circuits and Systems for Video Technology*, 14(1):21–30, 2004.

[7] W. Dong, Z. Sun, and T. Tan. Iris matching based on personalized weight map. *IEEE Trans. on Pattern Anal. Mach. Intell*, 33(9):1744–1757, 2011.

[8] E. Faramarzi, D. Rajan, and M. Christensen. Unified blind method for multi-image super-resolution and single/multi-image blur deconvolution. *IEEE Trans. on Image Processing*, 22(6):2101–2114, 2013.

[9] R. Gonzalea and R. Woods. *Digital image processing, 2nd ed*. Prentice Hall, New York, 2002.

[10] E. Guestrin and M. Eizenman. General theory of remote gaze estimation using the pupil center and corneal reflections. *IEEE Trans. on Biomedical Engineering*, 53(6):1124–1133, 2006.

[11] Z. He, T. Tan, Z. Sun, and X. Qiu. Toward accurate and fast iris segmentation for iris biometrics. *IEEE Trans. on Pattern Anal. Mach. Intell*, 31(9):1670–1684, 2009.

[12] K. Hollingsworth, K. Bowyer, and P. Flynn. The best bits in an iris code. *IEEE Trans. on Pattern Anal. Mach. Intell*, (6):964–973, 2009.

[13] X. Huang, L. Ren, and R. Yang. Image deblurring for less intrusive iris capture. In *CVPR*. IEEE, 2009.

[14] B. Kang and K. Park. Real-time image restoration for iris recognition systems. *IEEE Trans. on Systems, Man, and Cybernetics, Part B: Cybernetics*, 37(6):1555–1566, 2007.

[15] B. Kang and K. Park. Restoration of motion-blurred iris images on mobile iris recognition devices. *Optical Engineering*, 47:117202, 2008.

[16] A. Levin, Y. Weiss, F. Durand, and W. Freeman. Understanding and evaluating blind deconvolution algorithms. In *CVPR*. IEEE, 2009.

[17] X. Li, Z. Sun, and T. Tan. Comprehensive assessment of iris image quality. In *ICIP*. IEEE, 2011.

[18] J. Liu, Z. Sun, and T. Tan. Iris image deblurring based on refinement of point spread function. In *Chinese Conf. on Biometric Recognition*. Springer, 2012.

[19] Q. Shan, J. Jia, and A. Agarwala. High-quality motion deblurring from a single image. In *ACM SIGGRAPH*, pages 1–10. ACM, 2008.

[20] Z. Sun and T. Tan. Ordinal measures for iris recognition. *IEEE Trans. on Pattern Anal. Mach. Intell*, pages 2211–2226, 2009.